A Voltage Modulated DPC Approach for Three-Phase PWM Rectifier

Gui, Yonghao; Li, Mingshen; Lu, Jinghang; Golestan, Saeed; Guerrero, Josep M.; Quintero, Juan Carlos Vasquez

Published in:
I E E E Transactions on Industrial Electronics

DOI (link to publication from Publisher):
10.1109/TIE.2018.2801841

Publication date:
2018

Document Version
Accepted author manuscript, peer reviewed version

This article has been accepted for publication in a future issue of this journal, but has not been fully edited. Content may change prior to final publication. Citation information: DOI 10.1109/TIE.2018.2801841, IEEE Transactions on Industrial Electronics

A Voltage Modulated DPC Approach for Three-Phase PWM Rectifier

Yonghao Gui, *Member, IEEE*, Mingshen Li, *Student Member, IEEE*, Jinghang Lu, *Student Member, IEEE*, Saeed Golestan, *Senior Member, IEEE*, Josep M. Guerrero, *Fellow, IEEE*, and Juan C. Vasquez, *Senior Member, IEEE*

***Abstract*—In this paper, a voltage modulated direct power control for three-phase pulse-width modulated rectifier is proposed. With the suggested method, the differential equations describing the rectifier dynamics are changing from a linear time-varying system into a linear time-invariant one. In this way, the conventional feedback and feedforward controllers are applicable for the independent control of active and reactive powers. The proposed method is guaranteed that the closed system is globally exponentially stable. A feedback linearization method is also employed for generating the active power reference of inner loops. Finally, some experimental tests are conducted to verify its effectiveness.**

***Index Terms*—Exponential stability, linear time-invariant, rectifier, three-phase systems.**

I. Introduction

Three-phase rectifiers with the pulse-width modulation (PWM) are widely employed in different applications, particularly in interfacing distributed generation systems, drives of electrical motors, uninterruptible power supplies, etc. [1]. The control objectives for these applications are to maintain the DC-link voltage to a certain reference, supply a desired reactive power, and draw grid currents with the lowest possible harmonic distortion. The conventional control of the PWM rectifier is designed in a synchronous rotating reference frame, and a decoupled proportional-integral (PI) controller is applied for separately controlling d–q axes currents [2]. However, it suffers from a slow dynamical response.

To deal with such problem, different control methods have been designed [3]–[6]. Among them, methods based on the direct power control (DPC) have received great attention because it achieves the direct control of active and reactive power without using inner-loop current regulators [3]. A very brief review of recent advances in controlling rectifiers using the DPC method is presented in what follows.

A DPC technique based on the space vector modulation is proposed [5]. This control method, which does not require the extraction of positive and negative sequence components, results in low-THD line currents and eliminates double-frequency ripples under unbalanced grid conditions. In [7] and [8], a novel definition of reactive power has been applied in DPC to achieve an active power oscillation cancellation automatically with a simple structure. Providing a constant active power and sinusoidal grid currents even under an unbalanced grid are other advantages of this method. Recently, a model predictive control (MPC) based DPC technique has been applied to power converters [9]. The MPC-based DPC selects a voltage vector sequence and calculates duty cycles in every sampling period, which results in a constant switching frequency [10], [11]. The problem is that an incorrect voltage sequence selection may adversely affect the converter performance [12], [13]. MPC takes advantage of the discrete nature of the power converter, but the computation time is a critical issue.

In order to improve the DC-bus voltage dynamic performance with the consideration of the mismatched current or power disturbances, feedforward control techniques have been researched [14]–[17]. To improve reliability and decrease the cost of the load current sensor on the DC bus, load current observers are designed to identify the load current disturbance [18]–[20]. Recently, an extended state observer (ESO) based second-order sliding mode is proposed to improve the disturbance rejection ability [6]. Also, a proportional controller based ESO for the DC-link regulation is proposed to achieve the fast dynamics and high robustness. However, the nonlinear analysis and tuning of ESO are a bit complicated [21].

The motivation of this paper is to design a robust yet simple control strategy for the three-phase PWM rectifier. A voltage modulated DPC method is proposed, which has the following key features.

1) It changes the differential equations describing the dynamics of the three-phase PWM rectifier into a linear time-invariant (LTI) system;
2) It offers a simple way to design a traditional control method (feedforward and PI feedback) to obtain both a fast dynamic response and good steady-state performance without a phase-locked loop (PLL);
3) It is guaranteed that the closed system is globally exponentially stable;
4) It can be easily analyzed and designed by using conventional linear control techniques.

Finally, its effectiveness is verified through a real power converter prototype.

The rest of the paper is organized as follows. In Section III, the modeling of AC and DC side of the rectifier system

The authors are with the Department of Energy Technology, Aalborg University, 9220 Aalborg, Denmark (e-mail: yog@et.aau.dk; msh@et.aau.dk; jgl@et.aau.dk; sgd@et.aau.dk; joz@et.aau.dk; juq@et.aau.dk).

is presented. Section III describes the controller design and Section IV presents the experimental results with a 2.2-kW-VSC system. Finally, the conclusions are given in Section V.

II. Overview and Modeling of PWM Rectifier

A. AC-Side Modeling

Assuming the grid voltage is balanced, the grid voltage can be described as follows [22]:

$$\mathbf{v}_s = R_s\mathbf{i}_s + L_s\frac{d\mathbf{i}_s}{dt} + \mathbf{u}, \tag{1}$$

where $\mathbf{v}_s$, $\mathbf{i}_s$, $\mathbf{u}$ are the grid voltage vector, the input current vector, and the rectifier voltage vector, respectively. L_s and R_s are the filter inductance and resistance, respectively. We define the instantaneous active and reactive powers in the α-β frame as follows:

$$\begin{aligned} P &= \frac{3}{2}(v_{s\alpha}i_{s\alpha} + v_{s\beta}i_{s\beta}),\\ Q &= \frac{3}{2}(v_{s\beta}i_{s\alpha} - v_{s\alpha}i_{s\beta}), \end{aligned} \tag{2}$$

where P and Q are the instantaneous output active and reactive powers, respectively. $v_{s\alpha}$ and $v_{s\beta}$ indicate the grid voltages, and $i_{s\alpha}$ and $i_{s\beta}$ denote the injected currents in the α-β frame. By differentiating (2) with respect to time, the instantaneous active and reactive powers variations can be expressed as follows:

$$\begin{aligned} \frac{dP}{dt} &= \frac{3}{2}\left(i_{s\alpha}\frac{dv_{s\alpha}}{dt} + v_{s\alpha}\frac{di_{s\alpha}}{dt} + i_{s\beta}\frac{dv_{s\beta}}{dt} + v_{s\beta}\frac{di_{s\beta}}{dt}\right),\\ \frac{dQ}{dt} &= \frac{3}{2}\left(i_{s\alpha}\frac{dv_{s\beta}}{dt} + v_{s\beta}\frac{di_{s\alpha}}{dt} - i_{s\beta}\frac{dv_{s\alpha}}{dt} - v_{s\alpha}\frac{di_{s\beta}}{dt}\right). \end{aligned} \tag{3}$$

By assuming a nondistorted grid,, the following relationship could be obtained as

$$\begin{aligned} v_{s\alpha} &= V_s\cos(\omega t),\\ v_{s\beta} &= V_s\sin(\omega t), \end{aligned} \tag{4}$$

where V_s and ω are the magnitude and angular frequency of the grid voltage, respectively. By differentiating (4), the grid voltage variations can be expressed as follows:

$$\begin{aligned} \frac{dv_{s\alpha}}{dt} &= -\omega V_s\sin(\omega t) = -\omega v_{s\beta},\\ \frac{dv_{s\beta}}{dt} &= \omega V_s\cos(\omega t) = \omega v_{s\alpha}. \end{aligned} \tag{5}$$

Consequently, the dynamics of the instantaneous active and reactive powers could be obtained using from (1) to (5) as follows:

$$\begin{aligned} \frac{dP}{dt} &= -\frac{R_s}{L_s}P - \omega Q + \frac{3}{2L_s}(v_{s\alpha}u_\alpha + v_{s\beta}u_\beta) - \frac{3}{2L_s}V_s^2,\\ \frac{dQ}{dt} &= \omega P - \frac{R_s}{L}Q + \frac{3}{2L_s}(v_{s\beta}u_\alpha - v_{s\alpha}u_\beta), \end{aligned} \tag{6}$$

where u_α and u_β indicate the rectifier voltages in the α-β frame. Notice that (6) describes a time-varying system because the grid voltages multiply the rectifier voltages.

B. DC-Link Modeling

By neglecting the converter losses, the DC-link capacitor power variation can be expressed as

$$P_c = CV_{dc}\frac{dV_{dc}}{dt} = P_i - P_l, \tag{7}$$

where P_c, P_i, and P_l are the capacitor power, injected power form AC side, and consumed power by the load, respectively. C and V_{dc} are the DC-link capacitor and voltage, respectively. For the sake of simplicity, a resistive load is considered. Therefore, P_l can be expressed as

$$P_l = V_{dc}I_{dc}, \tag{8}$$

where I_{dc} is the current flowing into the DC load. Substituting (8) into (7) yields

$$\frac{dV_{dc}}{dt} = \frac{P_i}{C}\frac{1}{V_{dc}} - \frac{1}{C}I_{dc}. \tag{9}$$

Notice that (9) is a nonlinear system.

III. Controller Design for PWM Rectifier

To simplify the controller's design, an LTI system is needed as a system described in the d-q frame. To this end, we find a relationship between DPC model and system model in the d-q frame.

A. Voltage Modulated DPC

Let us define voltage modulated regulation (VMR) inputs as

$$\begin{aligned} u_P &= v_{s\alpha}u_\alpha + v_{s\beta}u_\beta,\\ u_Q &= -v_{s\beta}u_\alpha + v_{s\alpha}u_\beta. \end{aligned} \tag{10}$$

Notice that the VMR inputs are constant since the relationship between the VMR inputs and the rectifier voltages, as shown below, is the Park transformation.

$$\begin{bmatrix} u_P\\ u_Q \end{bmatrix} = V_s\underbrace{\begin{bmatrix} \cos(\omega t) & \sin(\omega t)\\ -\sin(\omega t) & \cos(\omega t) \end{bmatrix}}_{\text{Park Transformation}}\begin{bmatrix} u_\alpha\\ u_\beta \end{bmatrix}. \tag{11}$$

With the VMR inputs, the dynamics are transformed into an LTI system. To eliminate the coupling terms, the new control inputs are designed as follows:

$$\begin{aligned} u_P &= \frac{2L_s}{3}(\omega Q + \nu_P) + V_s^2,\\ u_Q &= \frac{2L_s}{3}(\omega P - \nu_Q), \end{aligned} \tag{12}$$

where ν_P and ν_Q are the new control inputs. With the VMR inputs, the dynamics (13) are transformed into a simple LTI system as follows:

$$\begin{aligned} \frac{dP}{dt} &= -\frac{R_s}{L_s}P + \nu_P,\\ \frac{dQ}{dt} &= -\frac{R_s}{L_s}Q + \nu_Q. \end{aligned} \tag{13}$$

This article has been accepted for publication in a future issue of this journal, but has not been fully edited. Content may change prior to final publication. Citation information: DOI 10.1109/TIE.2018.2801841, IEEE Transactions on Industrial Electronics

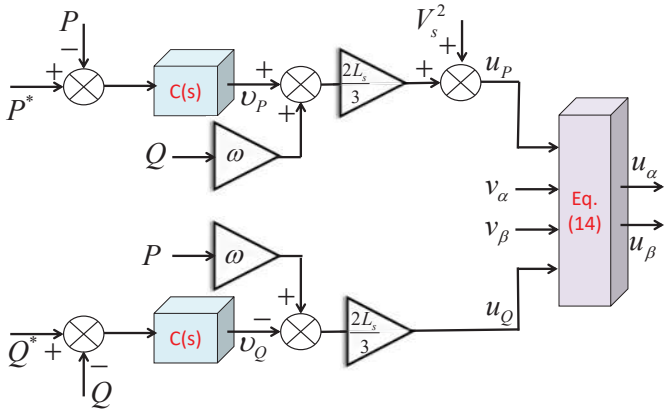

Fig. 1. The proposed $P\&Q$ controller setup.

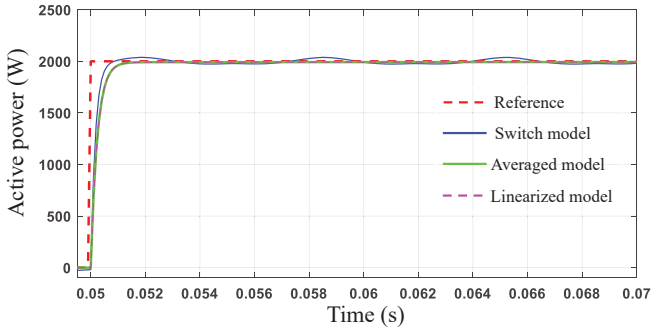

Fig. 2. Simulation results in comparison with averaged model and switched model.

Finally, using the inversion of (11), the original control inputs can be calculated as follows:

$$\begin{aligned} u_\alpha &= \frac{v_{s\alpha}u_P - v_{s\beta}u_Q}{V_s^2}, \\ u_\beta &= \frac{v_{s\beta}u_P + v_{s\alpha}u_Q}{V_s^2}. \end{aligned} \tag{14}$$

A controller for the active power can be constructed as shown in Fig. 1. A similar controller may be used for Q component.

Notice that, for $C(s)$, various control methods could be designed to satisfy the system's requirements. In this paper, we design PI controllers for both components,

$$\begin{aligned} \nu_P &= K_{p,P}(P^* - P) + K_{i,P}\int (P^* - P)dt, \\ \nu_Q &= K_{p,Q}(Q^* - Q) + K_{i,Q}\int (Q^* - Q)dt, \end{aligned} \tag{15}$$

where P^* and Q^* are the references of active and reactive powers, respectively. If the controller gains, $K_{p,P}$, $K_{i,P}$, $K_{p,Q}$, and $K_{i,Q}$ are designed as positive values, the closed-loop system remains exponentially stable. Substituting (15) into (13), the closed loop system can be obtained as follows:

$$\begin{aligned} \frac{dP}{dt} &= -\frac{R_s}{L_s}P + K_{p,P}(P^* - P) + K_{i,P}\int (P^* - P)dt, \\ \frac{dQ}{dt} &= -\frac{R_s}{L_s}Q + K_{p,Q}(Q^* - Q) + K_{i,Q}\int (Q^* - Q)dt. \end{aligned} \tag{16}$$

Differentiating (16) with respect to time yields

$$\begin{aligned} \ddot{P} &= -\frac{R_s}{L_s}\dot{P} + K_{p,P}(\dot{P}^* - \dot{P}) + K_{i,P}(P^* - P), \\ \ddot{Q} &= -\frac{R_s}{L_s}\dot{Q} + K_{p,Q}(\dot{Q}^* - \dot{Q}) + K_{i,Q}(Q^* - Q). \end{aligned} \tag{17}$$

Applying the Laplace transform to (17) gives

$$\begin{aligned} s^2P &= -\frac{R_s}{L_s}sP + K_{p,P}(sP^* - sP) + K_{i,P}(P^* - P), \\ s^2Q &= -\frac{R_s}{L_s}sQ + K_{p,Q}(sQ^* - sQ) + K_{i,Q}(Q^* - Q) \end{aligned} \tag{18}$$

or equivalently

$$\begin{aligned} \frac{P(s)}{P^*(s)} &= \frac{K_{p,P}s + K_{i,P}}{s^2 + (\frac{R_s}{L_s} + K_{p,P})s + K_{i,P}}, \\ \frac{Q(s)}{Q^*(s)} &= \frac{K_{p,Q}s + K_{i,Q}}{s^2 + (\frac{R_s}{L_s} + K_{p,Q})s + K_{i,Q}}. \end{aligned} \tag{19}$$

The characteristic polynomial of both these transfer functions, which describe the closed-loop dynamics of the active and reactive powers, is as

$$s^2 + \underbrace{(R_s/L_s + K_{p,P})}_{2\zeta\omega_n}s + \underbrace{K_{i,P}}_{\omega_n^2} = 0, \tag{20}$$

in which ω_n and ζ denote the natural frequency and the damping factor, respectively. Now, the proportional and integral gains may be selected by choosing a proper value for ω_n and ζ.

The damping factor ζ is the dominant factor in determining the damping of the dynamic response. A large value for this factor makes the dynamic response very damped and slow, and a small value makes it oscillatory and fast. To achieve a satisfactory compromise, most control texts recommend $\zeta = 1/\sqrt{2}$ [23]. Selecting the natural frequency ω_n also demands a tradeoff decision, but this time between the speed of dynamic response and noise immunity. Notice that the natural frequency is the dominant factor in determining the bandwidth of the control system. Therefore, a large value for that makes the dynamic response fast, but at the cost of degrading its noise immunity.

Once ζ and ω_n are selected, the control parameters can be calculated according to (20), as follows:

$$\begin{aligned} K_{i,P} &= \omega_n^2, \quad K_{p,P} = 2\xi\omega_n - \frac{R_s}{L_s}, \\ K_{i,Q} &= \omega_n^2, \quad K_{p,Q} = 2\xi\omega_n - \frac{R_s}{L_s}. \end{aligned} \tag{21}$$

Fig. 2 shows the step response of the switched model and averaged model. Notice that the closed-loop system is stable with proper controller gains, and then we can conclude that the closed-loop system is globally exponentially stable since it is an LTI system.

This article has been accepted for publication in a future issue of this journal, but has not been fully edited. Content may change prior to final publication. Citation information: DOI 10.1109/TIE.2018.2801841, IEEE Transactions on Industrial Electronics

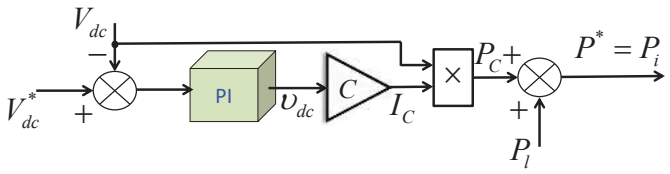

Fig. 3. DC-link controller block diagram.

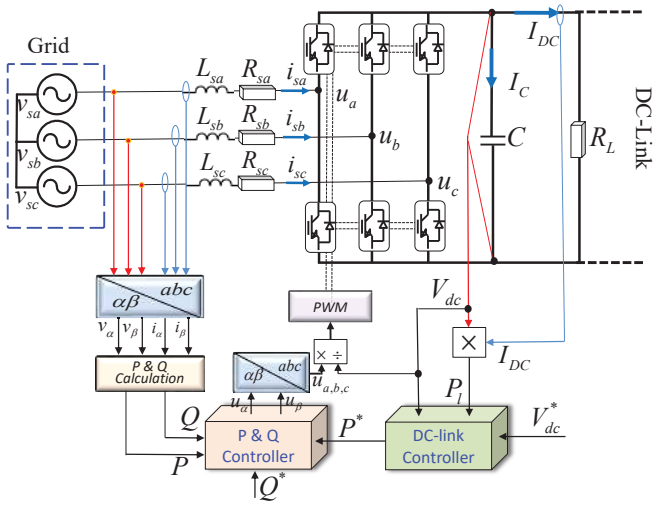

Fig. 4. Block diagram of the proposed method for the rectifier.

B. DC-Link Voltage Control

The main objective of the DC-link voltage is to regulate a constant reference value. Neglecting the losses, the injected power is designed as follows:

$$P_i = P_l + CV_{dc} \cdot \nu_{dc}, \tag{22}$$

where ν_{dc} is a new control input. Note that $CV_{dc} \cdot \nu_{dc}$ is equal to the power of the DC-link capacitor, P_C. The DC-link dynamics are changed into a simple LTI system as follows:

$$\frac{dV_{dc}}{dt} = \nu_{dc}. \tag{23}$$

For (23), various control methods can be applied to maintain a constant voltage. In this paper, a conventional PI DC-link controller is applied.

$$\nu_{dc} = K_{p,dc}(V_{dc}^* - V_{dc}) + K_{i,dc} \int (V_{dc}^* - V_{dc})dt, \tag{24}$$

where V_{dc}^* is the reference of the DC voltage, and $K_{p,dc}$ and $K_{i,dc}$ are controller gains (see Fig. 3). Notice that the generated control input, P_i, is the reference of the active power of the AC side. Finally, the whole block diagram of the proposed method is described as shown in Fig. 4. The DC-link controller enables the DC voltage to maintain a constant value, and the output of the DC-link controller, P^*, goes to the active power controller.

IV. Experimental Results

The effectiveness of the proposed method is verified by using a VSC (three-leg three-phase converter with an L filter),

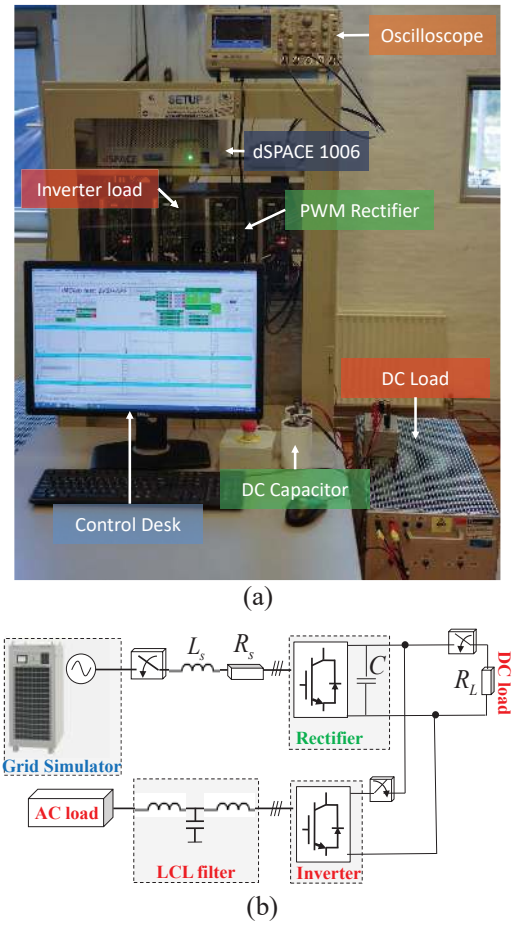

Fig. 5. (a) Experimental setup, (b) system architecture.

TABLE I
System Parameters Used in the Experiment.

Parameter	Value	Unit
Phase-to-phase RMS voltage	208	V
DC-link voltage, V_{dc}	500	V
Filter inductor, L_s	3.6	mH
Filter inductor, R_s	0.1	Ω
DC-link capacitor, C	1100	μF
Switching frequency, f_s	10	kHz
DC load, R_l	230	Ω

as shown in Fig. 5(a). The rectifier (Danfoss FC302 VLT 2.2kVA [24]) is connected to a programmable Grid Simulator, and two series-connected 2200μF/385V aluminum electrolytic capacitors in parallel with the DC-link. At the DC-link, the resister is connected as a DC load and another VSC with an AC load is emulated as an inverter load, as shown in Fig. 5(b). The detailed parameters used in the experiment are listed in Table I. The performance of the proposed method is compared with the traditional PI-based DC-link voltage controller and the PI plus feedforward method.

A. DC Load

As the first test, a disturbance is generated by connecting a 230 Ω resistor in the DC link. Fig. 6 shows the time response of the PI method, the PI plus feedforward method, and the proposed technique. It can be observed that the DC-link voltage and current using the proposed method has the smallest overshoot and fastest convergence time compared to other methods. This fact can be better visualized in Fig. 7, which shows the DC-link voltage response of all methods at the same time. It should be mentioned here that the simple PI method has the worst performance in this test.

B. Parameter Uncertainties

To test the robustness of the proposed controller to parameter uncertainties, its performance is evaluated in the presence of the inductance variation of the filter and capacitance variation of the DC-link capacitor. Fig. 8(a), (b), (c), (g), and (h) show the performance when the inductance of the filter in the control algorithm is set to 75% of the original value. Compared with Fig. 6, the tracking and steady-state performance of the proposed controller are not affected. Fig. 8(d), (e), (f), (i), and (j) show the performance when the capacitance of the DC-link capacitor in the control algorithm is set to 75% of the original value. The convergence time is a bit shorter than that without parameter uncertainty. Consequently, these mismatches have a small effect on the performance of the proposed controller. In addition, we insert 0.7% 5^{th} and 0.7% 7^{th} harmonics to the grid voltage by using the grid simulator to emulate the real grid. The DC load is suddenly connected to the DC link, in Fig. 9. The THD of the output currents is 2.5% when the THD of the grid voltage is 1.0%, as shown in Fig. 9(a) and (b). The tracking and steady-state performance are not affected by the harmonics, as shown in Fig. 9(c) and (f). Consequently, we can expect that the proposed method will be working well in the real grid.

C. Inverter Load

We also test a disturbance generated by connecting an inverter with an AC load in the DC link. At 0.5s, the inverter is suddenly connected to the DC link as shown in Fig. 10(e). Using the proposed method, the overshoot of the DC voltage is approximately 25V and the settling time is 0.2s. We can conclude that the proposed method is robust to the inverter load as well.

V. Conclusion

The proposed VM-DPC for the PWM rectifier is easy to control the active and reactive powers independently by using feedforward and feedback controllers. Experimental results show that the proposed method has not only fast transient response but also good steady-state performance. Under the proposed method, it is not hard to analyze and design for practicing engineers, since the system is changed into an LTI one. We show the proposed method is robust to the disturbance with the experiment since the closed-loop system is exponential stable.

References

[1] J. I. Leon, S. Kouro, L. G. Franquelo, J. Rodriguez, and B. Wu, "The essential role and the continuous evolution of modulation techniques for voltage-source inverters in the past, present, and future power electronics," *IEEE Trans. Ind. Electron.*, vol. 63, no. 5, pp. 2688–2701, 2016.

[2] M. Kazmierkowski and L. Malesani, "Current control techniques for three-phase voltage-source PWM converters: a survey," *IEEE Trans. Ind. Electron.*, vol. 45, no. 5, pp. 691–703, Oct. 1998.

[3] T. Noguchi, H. Tomiki, S. Kondo, and I. Takahashi, "Direct power control of PWM converter without power-source voltage sensors," *IEEE Trans. Ind. Appl.*, vol. 34, no. 3, pp. 473–479, 1998.

[4] M. Malinowski, M. Jasiński, and M. P. Kazmierkowski, "Simple direct power control of three-phase PWM rectifier using space-vector modulation (DPC-SVM)," *IEEE Trans. Ind. Electron.*, vol. 51, no. 2, pp. 447–454, 2004.

[5] Y. Zhang and C. Qu, "Direct power control of a pulse width modulation rectifier using space vector modulation under unbalanced grid voltages," *IEEE Trans. Power Electron.*, vol. 30, no. 10, pp. 5892–5901, 2015.

[6] J. Liu, S. Vazquez, L. Wu, A. Marquez, H. Gao, and L. G. Franquelo, "Extended state observer-based sliding-mode control for three-phase power converters," *IEEE Trans. Ind. Electron.*, vol. 64, no. 1, pp. 22–31, 2017.

[7] Y. Zhang and C. Qu, "Table-based direct power control for three-phase ac/dc converters under unbalanced grid voltages," *IEEE Trans. Power Electron.*, vol. 30, no. 12, pp. 7090–7099, 2015.

[8] Y. Zhang, J. Gao, and C. Qu, "Relationship between two direct power control methods for PWM rectifiers under unbalanced network," *IEEE Trans. Power Electron.*, vol. 32, no. 5, pp. 4084–4094, 2017.

[9] S. Vazquez, J. I. Leon, L. G. Franquelo, J. Rodriguez, H. A. Young, A. Marquez, and P. Zanchetta, "Model predictive control: A review of its applications in power electronics," *IEEE Ind. Electron. Mag.*, vol. 8, no. 1, pp. 16–31, 2014.

[10] S. Larrinaga, M. Vidal, E. Oyarbide, and J. Apraiz, "Predictive control strategy for DC/AC converters based on direct power control," *IEEE Trans. Ind. Electron.*, vol. 54, no. 3, pp. 1261–1271, 2007.

[11] P. Antoniewicz and M. P. Kazmierkowski, "Virtual-flux-based predictive direct power control of AC/DC converters with online inductance estimation," *IEEE Trans. Ind. Electron.*, vol. 55, no. 12, pp. 4381–4390, 2008.

[12] D.-K. Choi and K.-B. Lee, "Dynamic performance improvement of AC/DC converter using model predictive direct power control with finite control set," *IEEE Trans. Ind. Electron.*, vol. 62, no. 2, pp. 757–767, 2015.

[13] J. Hu, "Improved dead-beat predictive DPC strategy of grid-connected DC–AC converters with switching loss minimization and delay compensations," *IEEE Trans. Ind. Informat.*, vol. 9, no. 2, pp. 728–738, 2013.

[14] L. Malesani, L. Rossetto, P. Tenti, and P. Tomasin, "AC/DC/AC PWM converter with reduced energy storage in the DC link," *IEEE Trans. Ind. Appl.*, vol. 31, no. 2, pp. 287–292, 1995.

[15] M.-T. Tsai and W.-I. Tsai, "Analysis and design of three-phase AC-to-DC converters with high power factor and near-optimum feedforward," *IEEE Trans. Ind. Electron.*, vol. 46, no. 3, pp. 535–543, 1999.

[16] A. Yazdani and R. Iravani, *Voltage-sourced converters in power systems: modeling, control, and applications*. John Wiley & Sons, 2010.

[17] M. Davari and Y. A.-R. I. Mohamed, "Dynamics and robust control of a grid-connected VSC in multiterminal DC grids considering the instantaneous power of DC-and AC-side filters and DC grid uncertainty," *IEEE Trans. Power Electron.*, vol. 31, no. 3, pp. 1942–1958, 2016.

[18] R. Ghosh and G. Narayanan, "Generalized feedforward control of single-phase PWM rectifiers using disturbance observers," *IEEE Trans. Ind. Electron.*, vol. 54, no. 2, pp. 984–993, 2007.

[19] Z. Zhou, P. Unsworth, P. Holland, and P. Igic, "Design and analysis of a feedforward control scheme for a three-phase voltage source pulse width modulation rectifier using sensorless load current signal," *IET Power Electron.*, vol. 2, no. 4, pp. 421–430, 2009.

[20] C. Wang, X. Li, L. Guo, and Y. W. Li, "A nonlinear-disturbance-observer-based DC-bus voltage control for a hybrid AC/DC microgrid," *IEEE Trans. Power Electron.*, vol. 29, no. 11, pp. 6162–6177, 2014.

[21] J. Lu, S. Golestan, M. Savaghebi, J. C. Vasquez, J. M. Guerrero, and A. Marzabal, "An enhanced state observer for DC-link voltage control of three-phase AC/DC converters," *IEEE Trans. Power Electron.*, vol. 33, no. 2, pp. 936–942, 2018.

[22] P. Cortes, J. Rodriguez, P. Antoniewicz, and M. Kazmierkowski, "Direct power control of an AFE using predictive control," *IEEE Trans. Power Electron.*, vol. 23, no. 5, pp. 2516–2523, 2008.

This article has been accepted for publication in a future issue of this journal, but has not been fully edited. Content may change prior to final publication. Citation information: DOI 10.1109/TIE.2018.2801841, IEEE Transactions on Industrial Electronics

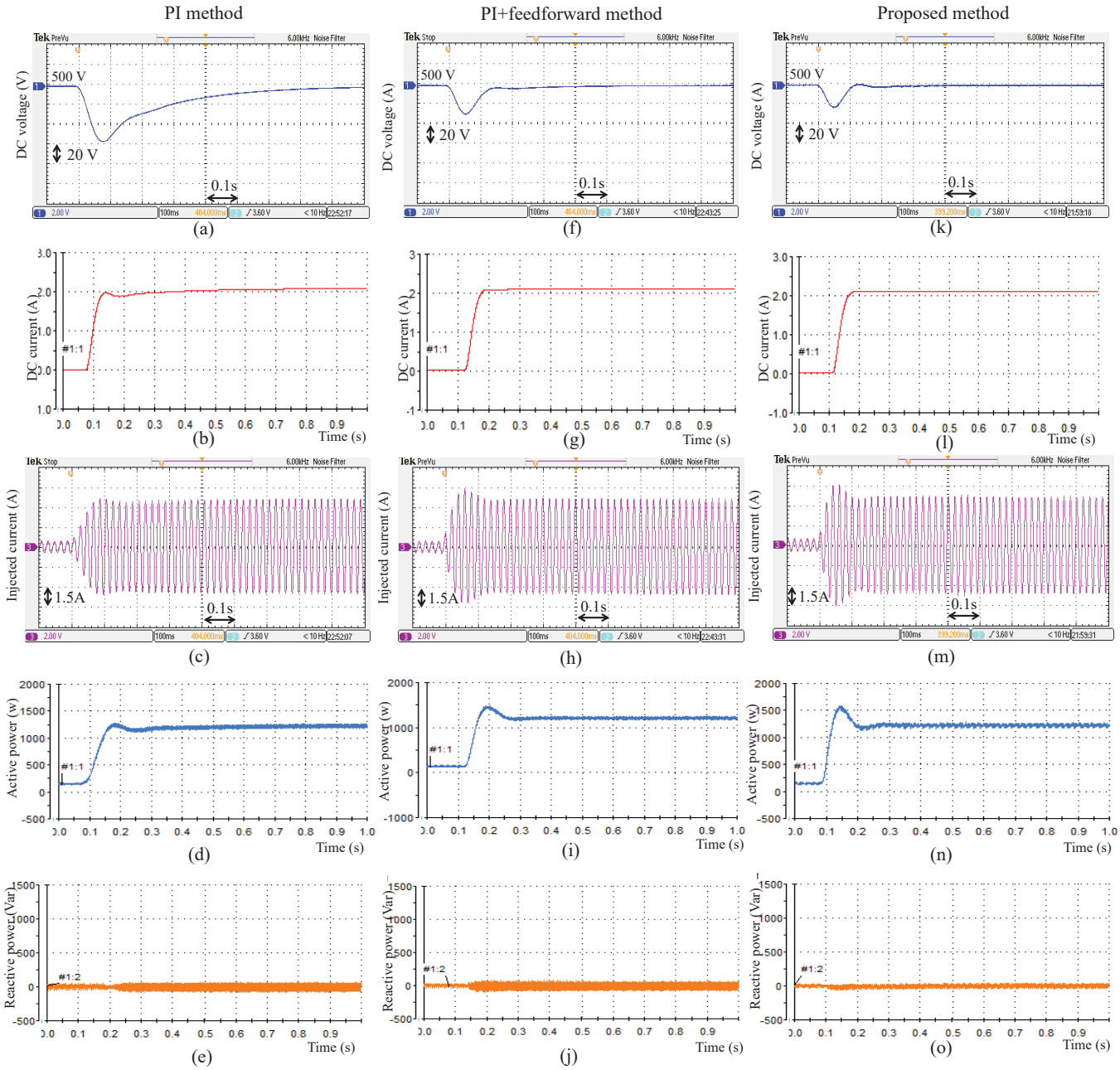

Fig. 6. Transient response and steady-state performance of the system under step change of the DC load. PI method: (a) DC voltage, (b) DC current, (c) injected current, (d) active power, (e) reactive power; PI plus feedforward method: (f) DC voltage, (g) DC current, (h) injected current, (i) active power, (j) reactive power; Proposed method: (k) DC voltage, (l) DC current, (m) injected current, (n) active power, (o) reactive power.

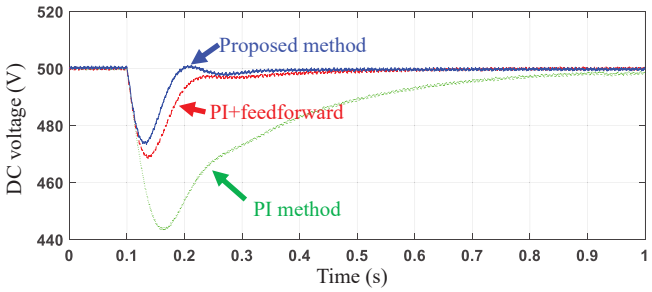

Fig. 7. Comparison of DC voltage.

[23] K. Ogata and Y. Yang, "Modern control engineering," 1970.
[24] Danfoss Drives. [Online]. Available: http://drives.danfoss.com/products/vlt/low-voltage-drives/vlt-automation-drive-fc-301-302/#/

This article has been accepted for publication in a future issue of this journal, but has not been fully edited. Content may change prior to final publication. Citation information: DOI 10.1109/TIE.2018.2801841, IEEE Transactions on Industrial Electronics

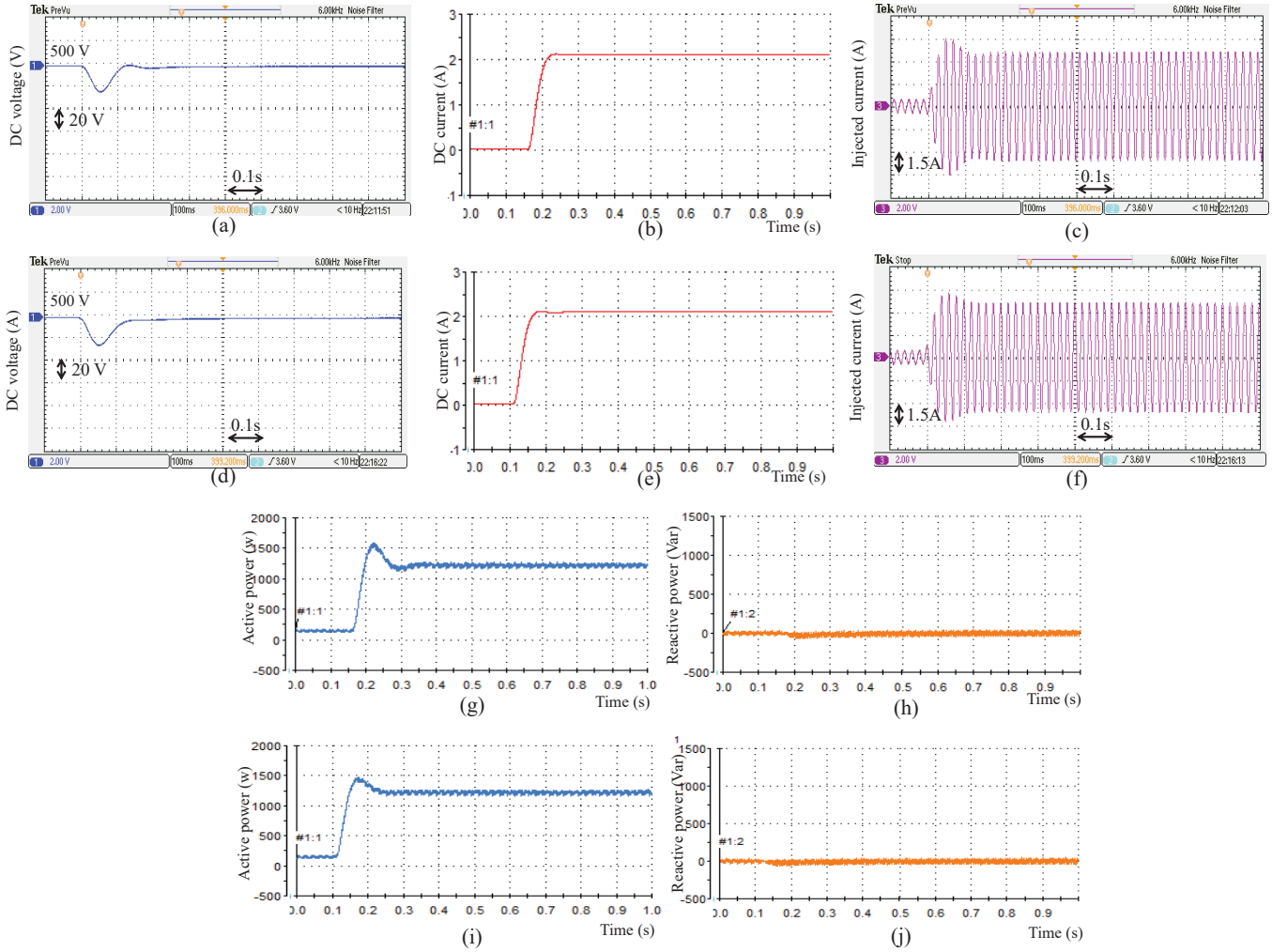

Fig. 8. Transient response and steady-state performance of the system under step change of the DC load when parameters of the controller are mismatched. $75\%L$: (a) DC voltage, (b) DC current, (c) injected current, (g) active power, (h) reactive power; $75\%C$: ((d) DC voltage, (e) DC current, (f) injected current, (i) active power, (j) reactive power.

Yonghao Gui (S'11-M'17) was born in Shenyang, China. He received the B.S. degree in automation from Northeastern University, Shenyang, China in 2009. He received the M.S. and Ph.D. degrees in electrical engineering from Hanyang University, Seoul, Korea in 2012 and 2017, respectively.

Since 2017, Dr. Gui has been working with the Department of Energy Technology, Aalborg University, Denmark, where he worked as a Postdoctoral Researcher at Microgrids Research Program (www.microgrids.et.aau.dk) from Feb. 2017 to Jan. 2018. His research interests include advanced control of power converter, microgrid, and renewable energy.

Mingshen Li (S'15) received the B.S. degree in electrical engineering from Chongqing University, Chongqing, China, in 2013, and the M.S. degree from Hunan University, Changsha, China, in 2016. He is currently pursuing the Ph.D. degree with Aalborg University, Aalborg, Denmark. His current research interests include primary control of converters, microgrids cluster system, and distributed generation systems.

Jinghang Lu (S'14) received the B.Sc. degree in electrical engineering from Harbin Institute of Technology, China, in 2009, and two M.Sc. degrees both in electrical engineering from Harbin Institute of Technology, China, in 2011, and University of Alberta, Canada, 2014, respectively. He is currently working towards the Ph.D. degree at the Department of Energy Technology, Aalborg University, Denmark. His research interests include uninterruptible power supply, microgrid, and control of power converters.

Saeed Golestan (M'11-SM'15) received the B.Sc. degree in electrical engineering from Shahid Chamran University of Ahvaz, Iran, in 2006, and the M.Sc. degree in electrical engineering from the Amirkabir University of Technology, Tehran, Iran, in 2009. He is currently working towards the Ph.D. degree at the Department of Energy Technology, Aalborg University, Denmark. His research interests include phase-locked loop and nonlinear filtering techniques for power engineering applications, power quality measurement and improvement, estimation of power system parameters, and microgrid.

This article has been accepted for publication in a future issue of this journal, but has not been fully edited. Content may change prior to final publication. Citation information: DOI 10.1109/TIE.2018.2801841, IEEE Transactions on Industrial Electronics

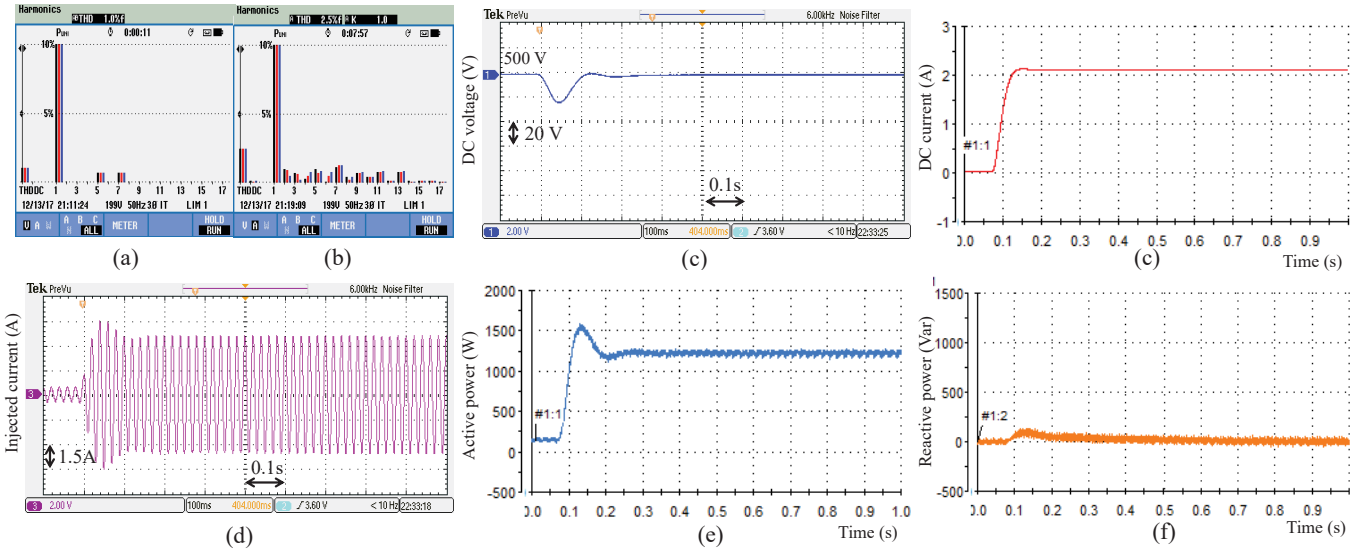

Fig. 9. Transient response of the system with the proposed method under step change of the DC load when the grid voltage has 5^{th} and 7^{th} harmonics. (a) voltage spectrum (THD=1.0%), (b) currents spectrum (THD=2.5%), (c) DC voltage, (d) DC current, (e) injected current, (f) active power, (g) reactive power.

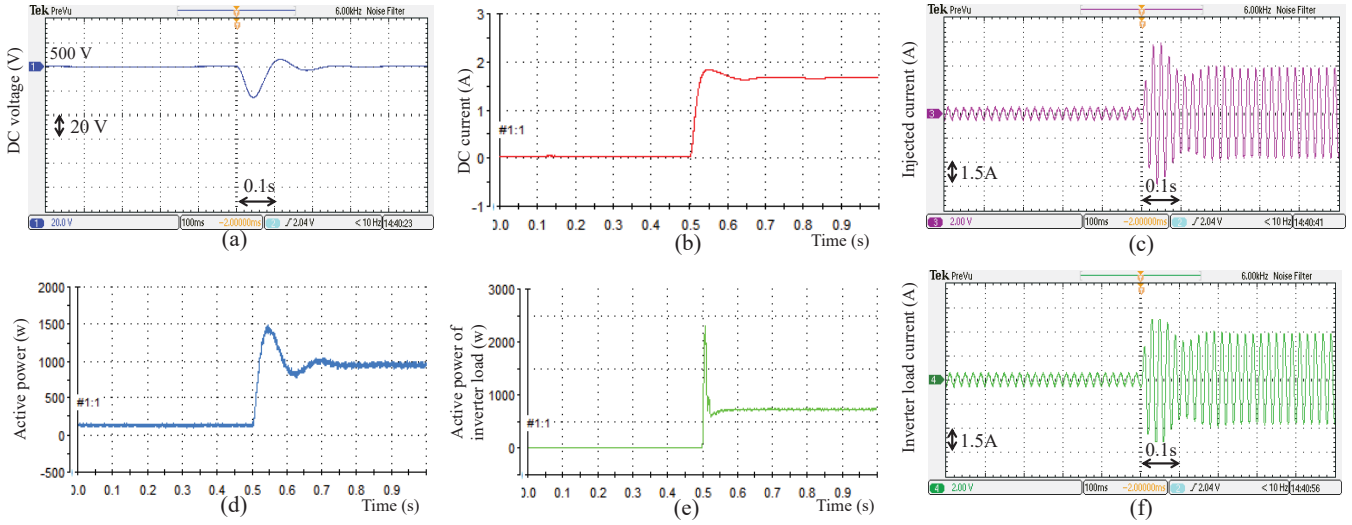

Fig. 10. Performance of the proposed method when the inverter is connected. (a) DC voltage, (b) DC current, (c) injected current, (d) active power of rectifier, (e) active power of the inverter, (f) output current of the inverter.

Josep M. Guerrero (S'01-M'04-SM'08-FM'15) received the B.S. degree in telecommunications engineering, the M.S. degree in electronics engineering, and the Ph.D. degree in power electronics from the Technical University of Catalonia, Barcelona, in 1997, 2000 and 2003, respectively. Since 2011, he has been a Full Professor with the Department of Energy Technology, Aalborg University, Denmark, where he is responsible for the Microgrid Research Program (www.microgrids.et.aau.dk). His research interests is oriented to different microgrid aspects. As well, he received the best paper award of the Journal of Power Electronics in 2016. In 2014, 2015, 2016, and 2017 he was awarded by Thomson Reuters as Highly Cited Researcher, and in 2015 he was elevated as IEEE Fellow for his contributions on "distributed power systems and microgrids."

Juan C. Vasquez (M'12-SM'14) received the B.S. degree in electronics engineering from UAM Manizales, Colombia, and the Ph.D. degree in automatic control, robotics, and computer vision from the Technical University of Catalonia, Barcelona, Spain, in 2004 and 2009, respectively. In 2011, He was Assistant Professor and from 2014 he is working as an Associate Professor at the Department of Energy Technology, Aalborg University, Denmark where he is the Vice Programme Leader of the Microgrids Research Program. His current research interests include operation, advanced hierarchical and cooperative control and the integration of Internet of Things into the SmartGrid. Dr. Vasquez is an Associate Editor of IET Power Electronics and in 2017 he was awarded by Thomson Reuters as Highly Cited Researcher.

Dr. Vasquez is currently a member of the IECSEG4 on LVDC Safety for use in Developed and Developing Economies, the TC-RES in IEEE Industrial Electronics, PELS, IAS, and PES Societies.